Available online at www.sciencedirect.com

ScienceDirect

Procedia CIRP 45 (2016) 363 – 366

www.elsevier.com/locate/procedia

3rd CIRP Conference on Surface Integrity (CIRP CSI)

Surface integrity of AISI 4140 after deep rolling with varied external and internal loads

D. Meyer[a,b]*, J. Kämmler[a,b]

[a]*Foundation Institute of Materials Science, Division Manufacturing Technologies, Badgasteiner Straße 3, 28359 Bremen, Germany*
[b]*University of Bremen and MAPEX Center for Materials and Processes, Bibliothekstr. 1, 28359 Bremen, Germany*

** Corresponding author. Tel.: +49 (0)421 218 51149; fax: +49 (0)421 218 51102. E-mail address: dmeyer@iwt.uni-bremen.de.*

Abstract

To achieve favorable surface and subsurface properties by means of compressive stresses, low surface roughness and strain hardened microstructures, deep rolling is a well-established manufacturing process. To gain a better understanding regarding the correlations between the rolling forces (external load), the resulting Hertzian stresses (internal material load), and the modification of surface and subsurface properties, in this paper, deep rolling parameters were varied in a defined way under consideration of the correlations between external and internal loads. It is shown that at identical external loads, different surface and subsurface properties may result due to a defined variation of the internal loads.

Peer-review under responsibility of the scientific committee of the 3rd CIRP Conference on Surface Integrity (CIRP CSI)
Keywords: Surface Integrity; Steel; Deep Rolling

1. Introduction

The functional performance of components, such as fatigue life, is strongly dependent on the surface integrity resulting from the applied manufacturing process. Processes with predominantly mechanical impact such as deep rolling are well-described to increase hardness, to induce compressive residual stress, and to change the microtopography [1]. Although the correlation between process parameters and resulting surface and subsurface properties is often discussed [2-4], the generation of defined changes in the functional material properties of components is still an iterative or experience-based process. To solve the inverse problem of generating a given desired surface integrity, a better understanding of mechanisms leading to a material modification is required. Byrne describes the need of an observation from within the workpiece to consider the effects (e.g. strain hardening) induced to the material while the tool influences the surface and subsurface of the workpiece [5]. This approach was further developed by Brinksmeier et al. to establish a mechanism-based description of machining processes and its resulting material modification [6]. For this, energy conversion and dissipation lead to a specific internal load in the material, resulting in a change of surface and subsurface properties (material modification) after machining [7]. According to this approach, deep rolling can be described as a moving pressure source, which induces internal mechanical loads such as stress and strain fields during the process (Fig. 1). The correlation of internal material load with the modification of state variables (residual stresses, hardness and microstructure) can be described as process signatures [7].

To characterize the internal material loads during deep rolling by means of equivalent stresses, Hertz allows for describing the pressure and contact conditions between two bodies of a defined geometry under elastic conditions [8,9]. In line with this approach, deep rolling of cylindrical workpieces can be assumed to correspond to the contact between to spheres [10], which allows the analysis of internal material loads. This approach was e.g. used in [11] to quantify the mechanical load in a cryogenically assisted deep rolling process.

This paper aims at establishing a changed perspective on the process from an external load oriented view, to an approach which focusses on the resulting internal material loads to predict the material modifications in surface and subsurface layers.

Peer-review under responsibility of the scientific committee of the 3rd CIRP Conference on Surface Integrity (CIRP CSI)
doi:10.1016/j.procir.2016.02.356

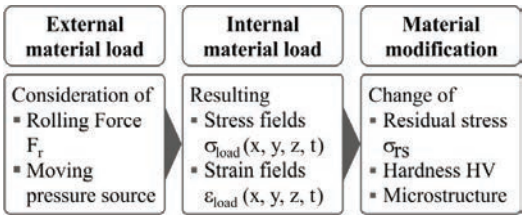

Fig. 1: transfer function for mechanical processes.

2. Experimental setup

The deep rolling experiments were performed on a conventional CNC turning lathe. As workpiece material, an AISI 4110 (42CrMo4) in a quenched and tempered state with hardness of 21 HRC was chosen. A spherical, hydrostatic guided deep rolling tool was used. Deep rolling of a cylindrical workpiece with an initial diameter of 60 mm is shown in Fig. 2.

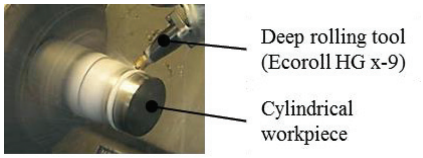

Fig. 2: experimental setup for deep rolling of cylindrical workpieces.

By choice of the deep rolling parameters, the external loads, the rolling force F_r, as well as the internal material loads resulting in a load dependent stress field are influenced. The basis for these investigations is the variation of tool diameter d_b and deep rolling pressure p_r, summarized in Table 1. To exclude the effect of multiple overlaps, a high feed was chosen leading to the separation of the single deep rolling tracks.

Table 1: chosen deep rolling parameters.

Parameters	Values
Ball diameter d_b	6 and 13 mm
Rolling pressure p_r	varied
Feed f	2.4 mm
Circumferential speed v_w	95 m/min

3. Parameter selection and results

The basis for the analysis of external loads is the deep rolling force F_r, whereas here, the equivalent stress σ_{eq} according to Hertz is used for the analysis of the internal material load. These values are subsequently related to the resulting residual stresses σ_{rs}.

3.1. External load oriented parameter selection

In many publications in the past, a conventional approach aims at the comparison of external loads. Thus, in the presented study, one part of the experiments was used to keep the rolling force constant. The rolling force F_r can be calculated by formula 1 as a result of the ball diameter d_b and the rolling pressure p_r [10]:

$$F_r = p_r \cdot \pi \cdot \left(\frac{d_b}{2}\right)^2 .$$

The deep rolling forces are kept at F_r = 1130 N to generate (supposedly) comparable process conditions for varied tool diameters. The resulting rolling pressure p_r for a tool diameter d_b = 6 mm and d_b = 13 mm is summarized in Table 2.

Table 2: chosen rolling pressure p_r resulting from constant rolling force F_r.

Rolling force F_r	Rolling pressure p_r	
	d_b = 6 mm	d_b = 13 mm
1130 N	400 bar	85 bar

Fig. 3 shows the residual stress depth profiles in feed direction for a constant rolling force F_r but for varied tool diameters d_b. The measured (XRD) residual stresses follow a similar trend, but vary regarding the maximum compressive residual stress $\sigma_{rs,max}$ and the depth of penetration. The constant force results in max. residual stress of -519 MPa for a tool diameter d_b = 6 mm in contrast to -575 MPa for d_b = 13 mm. The considerable deviation of the depth profiles indicates that the external load is not sufficient to predict the material modification.

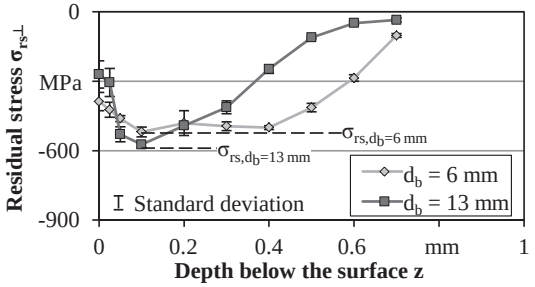

Fig. 3: residual stress depth profile σ_{rs} for varied tool diameters d_b on basis of constant rolling force F_r.

3.2. Internal material load oriented parameter selection

The target pursued in these experiments is a material-oriented way of choosing parameters for the generation of desired surface and subsurface properties. The operating rolling force F_r manifests in a stress field within the material. To describe the maximum stress just below the center of the tool, the Hertzian stress is taken into account based on the equations in [9]. This approach enables a qualitative approximation of internal material load for varied rolling parameters despite of limitations such as e.g. consideration of normal forces exclusively as well as a pure elastic material behavior [9].

For deep rolling of cylindrical workpieces, the contact between two spheres is considered. This case gives the best approximation between the effective contact of the deep rolling tool and the surface of the cylindrical workpiece. In order to generate a comparable uniaxial stress state, the equivalent stress is calculated according to von Mises. The depth profile of the equivalent stress σ_{eq} is presented in Fig. 4, while the applied parameters are summarized in Table 3.

Table 3: parameters for the analytical approach to define internal material loads according to Hertz.

Parameters	Cylindrical workpiece	Deep rolling tool
Material	AISI 4140	Ceramic
Geometry	Spherical	Spherical
Diameter	60 mm	6 or 13 mm
Poisson's ratio	0.30	0.33
Elastic modulus	210 GPa	305 GPa

The resulting depth profiles show a characteristic maximum stress below the surface. The level and the position of this maximum are dependent on the chosen deep rolling parameters. This effect can be used to establish a load oriented parameter selection for deep rolling processes. The profiles presented in Fig. 4 show an identical maximum of the equivalent stress $\sigma_{eq,max}$ for varied tool diameters d_b. This characteristic value $\sigma_{eq,max}$ enables an approach to compare the internal material loads of different process conditions and to correlate these internal material loads with the resulting material modifications based on the residual stress σ_{rs}.

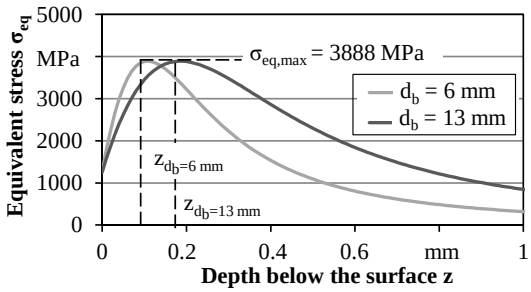

Fig. 4: equivalent stress depth profile σ_{eq} with constant maximum $\sigma_{eq,max}$ for varied tool diameters d_b.

Based on given fixed values for the maximum equivalent stress $\sigma_{eq,max}$, rolling pressures p_r can be determined for varied tool diameters d_b. The resulting rolling pressures p_r are given in Table 4.

Table 4: determined rolling pressure p_r resulting in constant maximum equivalent stresses $\sigma_{eq,max}$.

No.	Max. equivalent stress $\sigma_{eq,max}$	Rolling pressure p_r	
		d_b = 6 mm	d_b = 13 mm
1	1817 MPa		15 bar
2	2290 MPa		30 bar
3	2591 MPa		43 bar
4	3241 MPa	104 bar	85 bar
5	3888 MPa	180 bar	147 bar
6	4449 MPa	269 bar	220 bar
7	5077 MPa	400 bar	

The material modification is quantified based on the residual stress σ_{rs} in feed direction. An evaluation of residual stress profile in machining direction is not presented, since the residual stress in near-surface region is overlapped by plastic extension of pre-machining by turning processes. In Fig. 5, the analyzed residual stresses σ_{rs} for a maximum equivalent stress of $\sigma_{rs,max}$ = 3888 MPa is compared for tool diameters of d_b = 6 mm and d_b = 13 mm. Both depth profiles show identical development up to a depth below the surface of 100 µm as well as an identical maximum of the compressive residual stress $\sigma_{rs,max}$ = -539 MPa. However, in contrast to the internal material load, the measured depth of the maximum residual stress is identical at z = 100 µm for both diameters. The depth of the maximum equivalent stress for the smaller tool diameter (d_b = 6 mm) was z = 130 µm whereas the tool with a diameter of 13 mm showed the maximum in 180 µm depth. The penetration depth is strongly tool diameter-dependent. The residual stress value in the depths of the maximum equivalent stress values cannot be quantified due to the realized measurement intervals but based on the residual stresses for z = 100 µm and z = 200 µm, the values seem to vary within a range of -530 MPa.

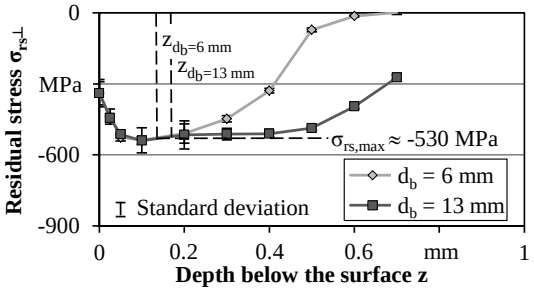

Fig. 5: residual stress depth profile σ_{rs} for varied tool diameters d_b based on constant maximum equivalent stress $\sigma_{eq,max}$ of 3888 MPa.

A similar result can be achieved for varied process parameters given in Table 4. Fig. 6 presents the maximum equivalent stress $\sigma_{eq,max}$ over the maximum compressive residual stress $\sigma_{rs,max}$. The maximum deviation occurs at an equivalent stress of $\sigma_{eq,max}$ = 3241 MPa and is about 8%. These investigations indicate that a correlation between the maximum of the equivalent stress $\sigma_{eq,max}$ and the resulting maximum residual stress $\sigma_{rs,max}$ is reasonable.

The observed deviations can be explained by the variation between the theoretical rolling force F_r and the achieved forces which are influenced by pressure loss in the system. The measured rolling forces indicate that a reduction of the max. equivalent stresses by 2.3 % (6 mm ball) or 7.2 % (13 mm ball) occurred during the experiments.

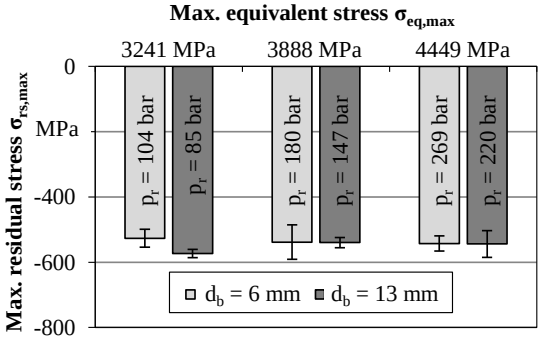

Fig. 6: resulting maximum residual stress $\sigma_{eq,max}$ for varied tool diameters d_b based on constant maximum equivalent stress $\sigma_{eq,max}$.

Fig. 7 presents the maximum equivalent stress $\sigma_{eq,max}$ over the maximum residual stress $\sigma_{rs,max}$ for different tool diameters d_b. Although the maximum equivalent stress $\sigma_{eq,max}$ increases continuously, the maximum compressive residual stress $\sigma_{rs,max}$ seems to constitute a maximum. As shown before in Fig. 6, the graphs show an almost identical tendency for equal equivalent stress $\sigma_{eq,max}$. Supplemented with correlations of additional internal material loads for varied tool diameters d_b, a polynomial trend can be recorded. This trend might be reasonable considering of an achievable maximum in residual stress before a disruption of material occurs due to high loads [2]. The presented correlations allow a process parameter independent view on the resulting surface integrity.

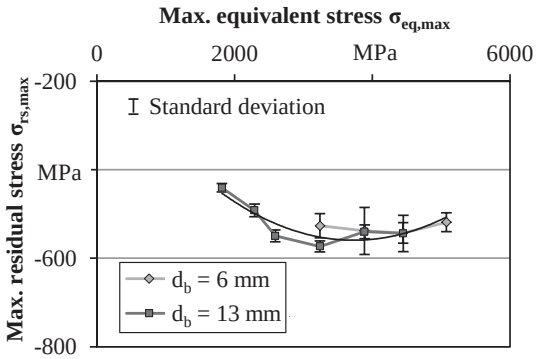

Fig. 7: correlation between maximum equivalent stress $\sigma_{eq,max}$ and resulting maximum residual stress $\sigma_{rs,max}$ – an approach for process signature.

4. Conclusion

In this study, deep rolling parameters were varied in defined ways to correlate the external load and the internal material loads with the resulting residual stresses. A consideration of a constant external load based on the deep rolling force F_r for varied tool diameters d_b showed poor comparability on basis of the residual stress depth profile.

Furthermore, an analytical approach by Hertz was used to describe the internal stress field below the surface of the material induced by deep rolling process. Based on the equivalent stress state, parameters were chosen, considering the internal loads of the material during machining. The maximum residual stress $\sigma_{rs,max}$ for varied tool diameters d_b, at a constant maximum equivalent stress $\sigma_{eq,max}$, showed an average deviation over all assessed surfaces of less than 3 %.

This investigation indicates the demand to generate process signatures for processes with mechanical impact as they allow for correlation of the internal material loads of a process with the material modifications. Regarding the inverse problem of producing desired surface and subsurface properties, the results allow conclusions to deduce required process parameters in deep rolling investigations. Fig. 8 presents the calculable ratio of maximum internal material load to maximum external load over the process parameters rolling pressure p_r and rolling force F_r. Considering the clear correlations between the ratio of stresses and the deep rolling parameters leading to this ratio, it will be possible to generate surfaces with desired residual stress states (inverse problem). Furthermore, validation of the observed effects at lower and higher equivalent stresses and varying tool diameter will be performed.

In addition, the depth effect of the process is of interest. A consideration of the penetration depth in the current analysis cannot be considered due to the measuring distances in the residual stress measurement. For this reason, the development of numerical approaches including elastoplastic effects is aspired for further investigations to gain extensive and detailed knowledge of the depth effect.

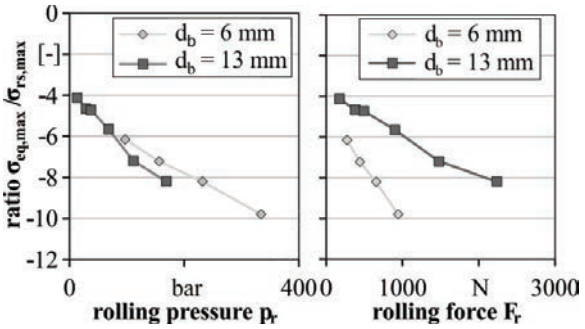

Fig. 8: the inverse problem – derivation of process parameters for generating a defined material modification.

Acknowledgements

The authors would like to thank the German Research Foundation (DFG) for funding the transregional Collaborative Research Centre SFB/TRR 136 “Process Signatures”, subproject F01.

References

[1] Nalla, R. K.; Altenberger, I.; Noster, U.; Liu, G. Y.; Scholtes, B.; Ritchie, R. O.: On the influence of mechanical surface treatments - deep rolling and laser shock peening - on the fatigue behavior of Ti-6Al-4V at ambient and elevated temperatures. Materials Science and Engineering A355 (2003) 216-230.

[2] Schulze, V.: Modern mechanical surface treatment. Wiley-VCH, Weinheim (2006).

[3] Altenberg, I.; Deep rolling – the past, the present and the future. Conference Proceedings ICSP (2005) 144-155.

[4] Trauth, D.; Klocke, F.; Mattfeld, P.; Klink, A.: Time-efficient prediction of the surface layer state after deep rolling using similarity mechanics approach. Procedia CIRP 9 (2013) 29-34.

[5] Byrne, G.: A new approach to the theoretical analysis of surface generation mechanisms in machining. Annals of the CIRP 41/1 (1992) 67-70.

[6] Brinksmeier, E.; Gläbe, R.; Klocke, F.; Lucca D. A.: Process signature – an alternative approach to predicting functional workpiece properties. Procedia Eng. 19 (2011) 44-52.

[7] Brinksmeier, E.; Klocke, F.; Lucca, D. A.; Sölter, J.; Meyer, D.: Process signatures – a new approach to solve inverse surface integrity problem in machining process. Procedia CIRP 13 (2014) 429 – 434.

[8] Hertz, H.: Über die Berührung fester elastischer Körper. Journal für die reine und angewandte Mathematik 92 (1881) 156-171.

[9] Johnson, K. L.: Contact mechanics. Cambridge University Press, Cambridge (1985).

[10] Röttger, K.: Walzen hartgedrehter Oberflächen. PhD, Shaker Verlag, Aachen (2003).

[11] Meyer, D.: Cryogenic deep rolling – An energy based approach for enhanced cold surface hardening. CIRP Annals – Manufacturing Technology 51 (2012) 543-546.